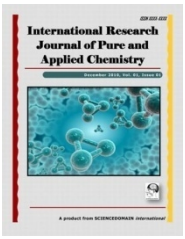

International Research Journal of Pure & Applied Chemistry
4(2): 144-158, 2014

SCIENCEDOMAIN *international*
www.sciencedomain.org

Application of Newton's Zero Order Caustic for Analysis and Measurement: Part III – Light Scattering

Antonio A. Garcia[1*], Luis Nuñez[2], Angel Lastra Miranda[3] and Vladimiro Mujica[4]

[1]School of Biological and Health Systems Eng., Arizona State University, Tempe, AZ, USA.
[2]Center for Green Manufacturing, University of Alabama, Tuscaloosa, AL, USA.
[3]School of Electrical, Computer and Energy Eng., Arizona State University, Tempe, AZ, USA.
[4]Department of Chemistry and Biochemistry, Arizona State University, Tempe, AZ, USA.

Authors' contributions

This work was carried out in collaboration among all authors. Authors AAG and LN designed the study and wrote the first draft of the manuscript. Authors ALM and AAG measured and analyzed the results. Authors LN and VM reviewed the optical ray tracing and managed the literature searches. All authors read and approved the final manuscript.

Original Research Article

Received 7th July 2013
Accepted 23rd September 2013
Published 13th November 2013

ABSTRACT

When light is incident upon a liquid suspension that has an oblate spheroid shape, the size and presence of particles can be determined by measuring light intensity exiting the sample or by imaging the scattered light using a digital camera. This dual analysis system is facilitated by Newton's zero order caustic formed within the sample, which creates a region of high intensity light inside the spheroid. Refraction of light exiting the spheroid directs a high percentage of scattered light near the zone of highest incident light intensity, which increases specific turbidity changes with particle size and facilitates analysis of gold nanoparticle plasmon resonance. Images taken with an ordinary digital camera at 90 degrees from the incident light can be analyzed using spatial autocorrelation in order to detect particle size.

**Corresponding author: Email: tony.garcia@asu.edu;*

Keywords: Newton's zero order caustic; gold nanoparticle; light scattering; autocorrelation; ray tracing.

ABBREVIATIONS

a = minor (orthogonal to light source) radius of a spheroid liquid sample; ACF = spatial autocorrelation function; b = major axis of a spheroid liquid sample; β = constant; ACF = autocorrelation function; C = concentration of species; χ = distance between spatial frequencies; D = diameter of particle; Γ = pre-exponential coefficient for spatial autocorrelation function; PTFE = polytetrafluoroethylene; I = intensity of light; I_o = incident intensity of light; N = number of particles; R = extinction coefficient in Beer-Lambert Law; τ = turbidity; x = distance across the optical path length; x_s = distance between the point source and the center of the water drop being illuminated.

1. INTRODUCTION

Accurately detecting the size and presence of particles is an essential need in many technologies including food processing, materials manufacturing, biotechnology, and medical testing [1]. Measuring the random changes in the intensity of light scattered from a suspension or solution is a widely used technique for determining particle size distribution and analyzing changes in particle sizes during aggregation, dissolution, crystallization, or coagulation events. Common optical state-of-the-art instruments for measuring particle size include dynamic light scattering (DLS), photon correlation spectroscopy (PCS), nephelometry, and quasi-elastic light scattering (QELS). All of these techniques involve illuminating particles with monochromatic, collimated light and employ planar or cylindrical sample chamber geometry between the source laser and the detecting unit. In scattering media, the intensity of scattered light collected at different angles is a function of particle size, the wavelength of incident light, and the relative refractive index of the liquid and suspended particles. The authors are not aware of any scattering-based, optical analysis systems that modify light entering the sample chamber to form an optical caustic, which is a convergence of light rays resulting in zones of high light intensity.

In the first two parts of this 3-part series, the detection of solutes in water by absorbance and by fluorescence using light formed into an optical caustic within the sample is discussed and experimental results are compared with measurements from conventional systems. An optical caustic consists of an envelope of light rays that exhibits complex wave effects. This concentration of light creates a boundary between regions in which the light intensity transitions greatly. On one side there is an intensity decreasing rapidly to zero, and on the other there are interference fringes similar to what is observed for two coherent superimposed beams. Inside the caustic, there are wave fronts that interfere to produce the fringes [2].

Developing a light scattering system based on optical caustics has the potential to lower equipment costs and power consumption due to refraction of scattered light as well as the intensity increase from the overall refraction of incident light. The growing use of nanoparticles in diagnostic methods and the interest in environmental sampling using portable and rugged systems are other motivating factors. This paper explores light scattering of gold and polystyrene nanoparticles using a low power LED source, with light focused by the sample as a caustic [3-6], and detected using off-the-shelf electronics or a cell phone camera. Results and observations are compared to ray tracing predictions and

published light scattering theories. Experimental results are described to help point towards ways that the optical platform could be configured with different detection systems and used in a variety of applications.

2. MATERIALS AND METHODS

2.1 Sample Stage

The sample stage employed a PTFE coated slide with 30 wells of 3 mm diameter (Tekdon Inc., Myakka City, FL), which pinned drops of 120 or 160 microliters of the aqueous particle suspension. The colloidal sample formed an oblate spheroid on the slide, and is held in place without a sample container. Each multi-well slide can measure 5 different liquid suspensions and each position can be used for multiple tests of the same colloidal suspension. At room temperature, the optical signal changes very slowly due to evaporation since the aqueous drop is pinned into a spheroid shape rather than allowed to spread to form a high surface area thin film, which would evaporate relatively quickly. The spheroid shape of the samples was characterized using Image J (http://rsbweb.nih.gov/ij/) and found by edge analysis and measurement to have the ratio of 1.5 for the simple suspensions studied, due to the balance between pinning, gravity, and surface tension. For this initial study of Newton's zero order caustic, an open-air sample avoids the need to correct for refraction of light from a curved sample container.

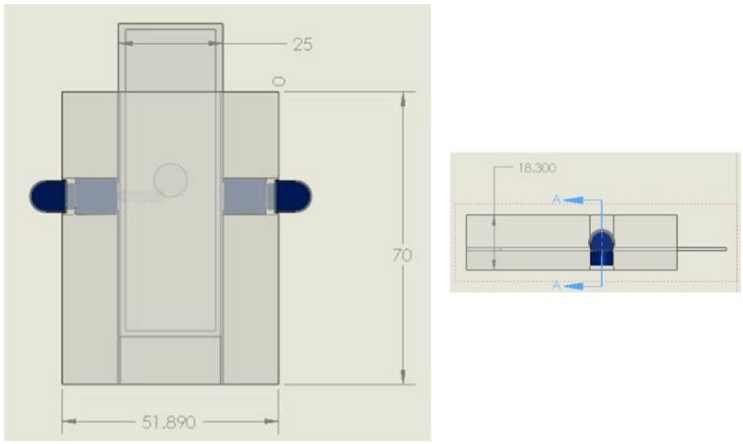

Fig. 1. Sample stage schematic diagram is shown. Photodiodes are drawn in blue. All measurements are in millimeters. A 25 mm wide, 30-well slide is used instead of the single well slide depicted. The sample droplet is placed in the center of the slide, and there are five positions or samples that can be held per slide

2.2 Nanoparticles

Gold nanoparticles (10, 40, and 100 nm diameters) were purchased from BBI Solutions (Cardiff, UK).Gold nanoparticles were used at the concentrations (particles/ml) of 5.7×10^{12} (10 nm), 9.0×10^{10} (40 nm) and 5.6×10^{9} (100 nm). Calculated extinction coefficients at the plasmon peak resonance for 10, 40, and 100 nm gold particles can be found in the literature as 0.5, 3.8, and 7 respectively [7].Scattering cross sections for 10, 40, and 100 nm diameter

gold particles calculated by Mie theory can be found in the literature as 0.01, 13, and 10,000 nm^2 respectively [8].

Functionalized polystyrene nanoparticles (carboxylate or amino, 180, 200, 500, 750, 1000, and 2000 nm diameters) were purchased from Polysciences Inc. (Warrington, PA). Measurements were made at a particle concentration of 0.025% for the speckle analyses. A series of 10 dilutions were used for specific turbidity measurements as explained in Section 2.5 below.

2.3 Light Scattering Measurements

Light emission and photodetection were accomplished using a matched set of photodiodes with internal micro-lens and PBT housing (Industrial Fiber Optics, Tempe, Arizona): Red, 640 nm peak wavelength and Blue, 430 nm peak. The photoemitter was powered by a standard constant voltage DC circuit, based on the manufacturer's recommended value of 4.5 Volts at 35 mA. The photodetector was connected to an operational amplifier (LF351, Fairchild Semiconductor, San Jose, CA) in open circuit mode using reverse bias. Volt or panel meters were used to measure the voltage at the photodetector for static measurements. When connected to the operational amplifier circuit, the meters were tested to read 0.00 with total light blockage. Panel meters were tested with an Omega handheld multimeter using simple DC circuits for 0.1, 0.5, 1, and 7 volts. The linearity with voltage for both panel and multimeter was within 4% agreement. Voltage measured for a particular suspension was compared to the voltage for pure water as a reference. Alignment was accomplished by visual inspection of the beam on the barrel of the detector. This was found to be sufficiently accurate for the range of experiments conducted.

Detection of 90 degrees scattered light was conducted using an HTC Incredible 2 Android cell phone camera to acquire images. The ImageJ software program was used after the image was recorded to measure pixel intensity profiles for determining the spatial autocorrelation function (ACF) or integrated density in order to calculate scattering intensity. An average pixel intensity for each profile was used prior to calculating ACF in order to normalize the data. The camera was rested on a cradle and heldvertically between 4-5 cm from the sample so that the camera lens and the droplet were at the same height. Images were taken by pointing the cradle orthogonal to the direction of the droplet illumination. The system was found to give reproducible images and data even if the distance between the sample and camera was varied between 4-5 cm, as long as each image was analyzed at a constant distance for the particular image series. In order to reduce interference from ambient light, a black colored light box was lowered over the camera and sample stage after setting the camera timer for a 5 second delay.

The data are presented here after extensive replicate measurements were made using different sample slides, samples, images, and photodiode instruments. In order to present the information clearly, replicate data or error bars are not given in the graphs. Also, replicate images are not provided but instead representative images are given. Throughout the experiments, we recorded variations in the photodiode detector signals of 4%. The imaging data showed more variation due to differences in background light that caused some variation in the speckle images. Overall, the maximum variation in the imaging analysis was found to be 7% for the measurements taken.

2.4 Measurement by Light Extinction

Results using the photodiode detection system were compared to light extinction (described phenomenologically as absorbance readings) measurements taken by a spectrophotometer (model USB2000 Miniature Fiber Optic Spectrometer, Ocean Optics). This spectrophotometer accepts incident radiation transmitted through a single-strand optical fiber (400 μm fiber diameter, UV/VIS Laboratory-grade Patch Cord Optical Fiber Assembly, Ocean Optics) and disperses it via a fixed grating across a 2048-element linear CCD array detector. The operating software (SpectraSuite, v. 2.0.109, Ocean Optics) runs on a Mac Pro laptop (Apple, Cupertino, CA). An achromatic collimating lens (350-2000 nm) (model 74-ACR, Ocean Optics) was used to collect the incident light, which is then transmitted through the optical fiber to the grating. Plastic or quartz cuvettes were used with an optical path length of 1 cm. Spectra were taken based on an average of 50 scans at 20 milliseconds per scan.

For time dependent measurements, a DAQ Data Logger Model LGR-5327 was used to acquire voltage readings at 10 Hz from the operational amplifier detector circuit. Due to the signal amplification, there is a randomly oscillating noise level of 0.2 volts during these measurements. However, the overall signal measurement was on the order of 3-5 voltsand the trend with gold nanoparticle coagulation was at least a difference of 1 V. Also, the much lower frequency response during experiments with sodium chloride addition was clearly distinguishable from the higher frequency oscillations.

2.5 Calculation of Light Scattering Properties

Specific turbidity was calculated by first determining the turbidity τ from the photodiode detector as a function of particle concentration for ten dilutions from 0.025 Wt% to 0.1% wt%. Turbidity was calculated as the ratio of the log of the voltage measured for a given sample divided by the voltage for pure DI water. Next, the values of turbidity were divided by concentration and graphed as a function of concentration. The limiting slope at low concentration was extrapolated to be the specific turbidity $\left({}^{\tau}/_{C}\right)_{0}$.

Twenty separate plot profile datasets were collected using ImageJ for images with 200, 500, 750, 10000, and 2000 nm polystyrene suspensions. For the droplets, the plot profile data was collected from the top of the droplet to the base at the center. For the quartz cuvettes, plot profiles were collected away from the reflection zone but near the center of the cuvette. Each plot profile consisted of at least 300 data points. For each plot profile, the intensity values were normalized using the average intensity prior to computing the Autocorrelation information using the online software tool http://www.wessa.net/rwasp_autocorrelation.wasp/. The natural log of the autocorrelation values were plotted as a function of distance interval and the initial slope was calculated.

3. RESULTS AND DISCUSSION

3.1 2-D Ray Tracing

In Parts I and II of this three part series, ray tracing was used to illustrate how light from a LED is focused into a caustic within the sample due to refraction. In Fig. 2, an image of 100 nm diameter gold particles suspended in water is shown along with a ray trace for a point

source and a spheroid of aspect ratio 1.5 that contains only water. Due to light scattering, the gold nanoparticles outline the concentration of light within the sample in a manner similar to dust illuminating the path of a projector beam. Gold nanoparticles of 10 and 40 nm diameters have one million and one thousand fold lower scattering cross section, respectively, than 100 nm gold particles, making the 100 nm size particularly useful for illustrating the formation of Newton's zero order caustic. Before exploring light detection using 90 degree imaging, it is instructive to understand how light exiting the sample at 0 degrees can be monitored in terms of specific turbidity or as light extinction.

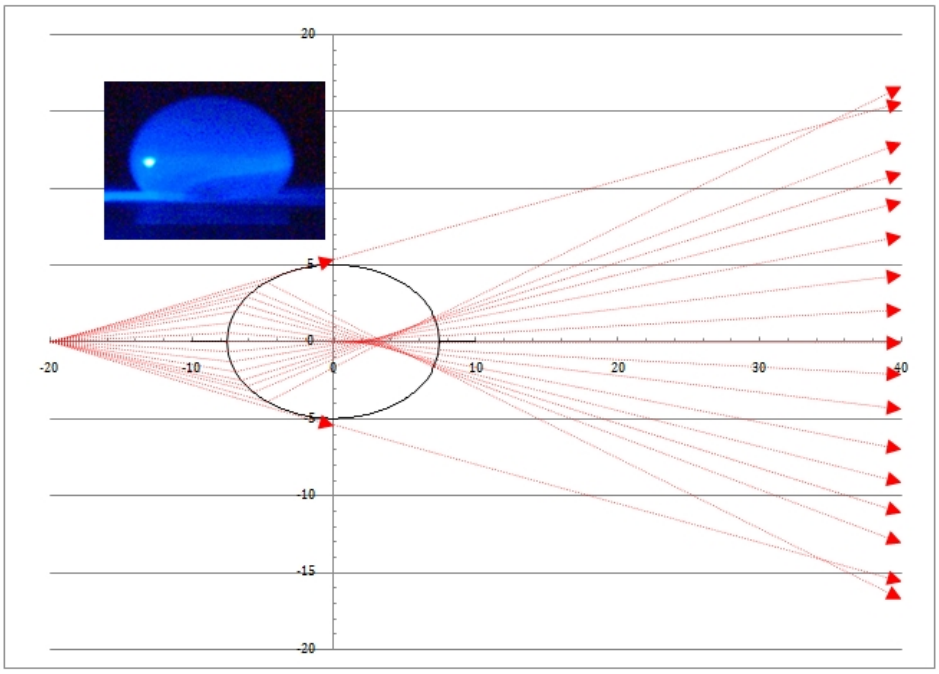

Fig. 2. Ray tracing for a point source of light that is refracted within a spheroidal (b/a ratio of 1.5) droplet containing only water, due to Newton's zero order caustic. The equations used for the ray tracing are based on the work of Lock and McCollum [9]. The insert is an image taken using a cell phone camera of a 100 nm gold particle aqueous suspension which illuminates the light rays through scattering and illustrates that the ray tracing is a reasonable representation of how light is concentrated in the experimental platform used to collect data. The bright spot seen in the insert is a reflection of the light used for illumination. The widest dimension of the drop shown in the image is 3.7 mm

Measuring the attenuation of light that passes through the oblate spheroid is similar to a turbidity measurement, but the generation of a caustic enhances the signal as changes occur in the particle shape and size. Also, due to refraction, there is information acquired in a zone of the sample near the caustic focus for light scattered at small and near 90 degree angles. First, a review of data and theory based on the Mie equations for light scattering is useful to explain the intrinsic difference between light scattering from caustics in oblate spheroids versus standard planar measurements of turbidity and light scattering using cuvettes.

3.2 Forward Scattering

The fractional decrease in a beam of light due to scattering can be stated in an analogous way to the Beer-Lambert law $-\frac{dI}{I} = RNdx$ and the turbidity can be defined as $\tau = \frac{\ln\left(I/I_0\right)}{L}$ where L is the path length. In order to represent the intensity data as a function of particle concentration, the specific turbidity at infinite dilution is employed as the dependent variable $\left(\tau/C\right)_0$, and it is proportional to the Mie scattering coefficient defined by Bateman and colleagues [10]. The specific turbidity was calculated using an exponential curve fit of the relative voltage readings from the photodiode detector using polystyrene suspensions (see Fig. 3). Bateman and colleagues [10] and Tabibian and colleagues [11-16] conducted a series of measurements using different wavelengths and polystyrene particles and developed simplified equations that correlate well with Mie theory to predict specific turbidity [10].

Fig. 3 compares cuvette and oblate spheroid samples with the data by Bateman and colleagues [10] and the theoretical equation by Tabibian, Heller, and Epel [13] using 650 nm light. Agreement among the cuvette data, published data by Bateman, and the theoretical curve by Heller (Fig. 3) is reasonable both in the magnitude of the specific turbidity and the overall shape of the trend with respect to particle diameter. However, the oblate spheroid sample clearly measures higher specific turbidity at all particle sizes. Moreover, the trend of the data for particles above 200 nm diameter diverges markedly from the rest of the data and from Mie theory as well. The result of this behavior is that the optical system measures particle differences or size changes more sensitively for this range than a standard turbidity meter.

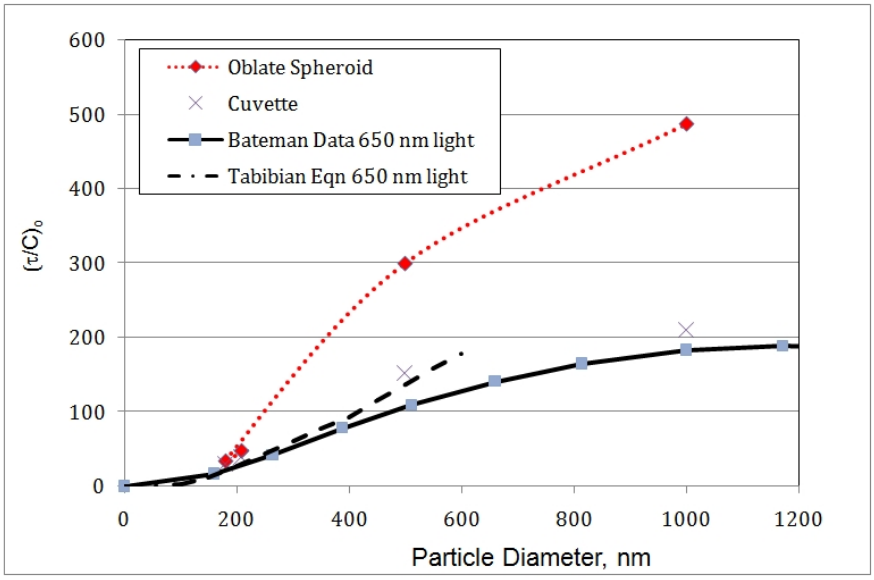

Fig. 3. Comparison of forward scattering, using specific turbidity, for the oblate spheroid and cuvette illuminated by 640 nm light with published data and theory [10-16]. Measurements were performed using polystyrene particle suspensions. Each data point is based on fitting data from ten dilutions using triplicate measurements for each dilution. The oblate spheroids had an aspect ratio of 1.5

3.3 Determining Particle Size

Since, as seen in Fig. 1, the optical platform also accommodates imaging of the suspension at 90 degrees form the incident light source, a series of images for different particle sizes were analyzed following the work of Cichea [17], Carnibella and colleagues [18], and Carvalho and colleagues [19] who suggest that a spatial autocorrelation function (ACF) analysis can yield particle size information in a matter analogous to dynamic light scattering. After the spatial ACF was determined, it was interpreted using the following equations:

$$ACF = be^{-\Gamma c} \tag{1}$$

$$\Gamma \mu \frac{1}{D} \tag{2}$$

Where β is a constant, χ is the distance interval between spatial frequencies, and D is the diameter of the particles. This method parallels the use of ACF in dynamic light scattering and generally conforms to the equations used by Carvalho and colleagues [19] and Cichea [17].

Analyzing images at dilutions below 0.025 Wt%, and for sample sizes of 120 and 160 microliters, ACF was calculated from the pixel intensity variation normalized by subtracting the average intensity. The ACF curves were plotted and fitted to Equation (1) in order to obtain values of the parameter Γ. An example of data from a series of 160 microliter samples of polystyrene particle diameter is graphed in Fig. 4. There is a reasonable linear correlation between particle sizes of 200-1000 nm, but the 2000 nm particle data is near the value for 1000 nm polystyrene particles and the linear relationship does not hold for that size interval. This overall trend in the data is very similar to what was observed by Carvalho and colleagues [19] and understandable since there is a marked increase in forward scattering for particles at 2000 nm. Moreover, the anisotropy factor calculated using Mie Theory for 1000 and 2000 nm particles are essentially the same. Carvalho [19] and Piederriere [20] both show that this results in a very small speckle size difference in the range of 1000-2000 nm and hence a small difference in the parameter.

In order to detect changes in forward scattering via Newton's zero order caustic, a simple experiment was performed to verify that 1000 nm particles can be distinguished from 2000 nm particles. Using the fiber optic spectrometer and starting with a suspension of 1000 nm diameter particles, there is a nearly 20% increase in signal when 2000 nm diameter particles were added at a concentration of 100 nanograms/ml particles (a 100-fold lower concentration than the 1000 nm sample) [21]. The same experiment with a cuvette instead of the oblate spheroid, while yielding a slight increase in signal, was within the margin of error and hence could not conclusively indicate the presence of the 2000 nm diameter particles at this relatively low concentration [21]. Why these results occur is discussed in the next section.

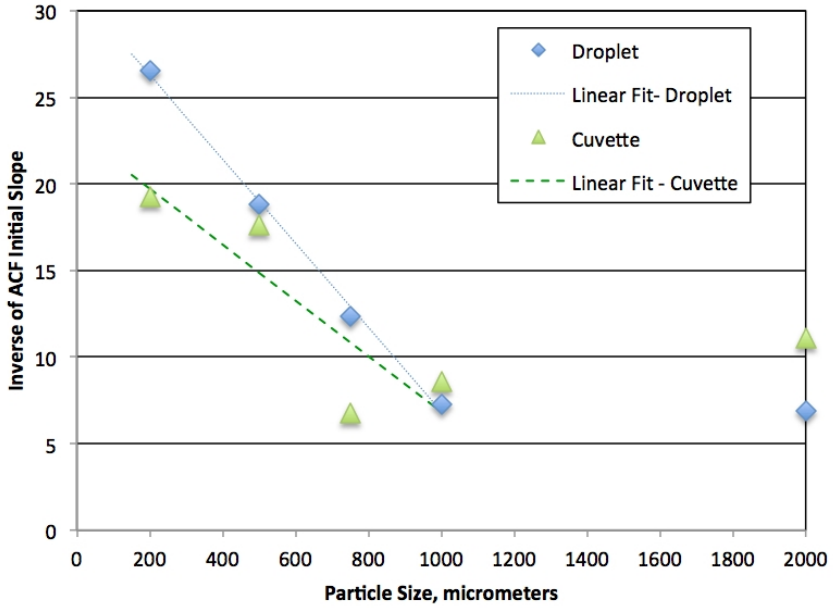

Fig. 4. Results of spatial autocorrelation calculations of droplet and cuvette suspensions using cell phone images of 90 degree scattering of 430 nm light andaqueous suspensions of polystyrene particles. The cuvette data has more variation than the droplet data because the sample stage used was not optimized for cuvette optics and there was some reflection from the photodiode incident light in the speckle images analyzed

3.4 Comparison between Cuvette and Caustic

In order to gain insight into the role of refraction in the enhanced sensitivity for forward scattering, ray tracing calculations for a cuvette, spherical sample, and oblate spheroid for rays entering at the centerline of the sample that undergo a scattering event were performed. The objective of these calculations is to illustrate graphically the maximum scattering angle that could still reach a detector positioned at the opposite end of the sample. For the cuvette, a standard detector window was assumed to be next to the opposite face of the cuvette, which is a reasonable configuration for spectrophotometers. For the spherical and oblate spheroid samples, a similar size window was placed at a distance 4d (or 4a for the ellipse cross section) relative to the center of the sample. Angles beyond the critical angle within the sphere or oblate spheroid lead to reflection, and those rays are not considered in this theoretical analysis. Also, the refraction of light due to the thin wall of the cuvette was assumed to be negligible.

Fig. 5 shows the results of the ray trace calculation in terms of maximum angle of scatter that can reach the detector as a function of fractional distance across the sample. There are two distinct features in the curves shown in Fig. 5. First, for the curved samples there is a region where the maximum angle of scattered light reaching the detector reaches a peak at a zone within the sample whereas for the cuvette the relationship is a monotonically increasing function of path distance. Secondly, the sphere and oblate spheroid curves show complex results at the curves' maxima, which is depicted graphical as a region bounded by a

dashed or dotted line. If light is scattered in this zone, there is a bifurcation in the function of path distance versus maximum scattering angle collected due to refraction, and hence a "blind spot" occurs where scattered light of certain angles cannot enter the detection zone. In other words, there can be a zone that has small angle scattering (0-8 degrees) and 80-90 degree scattering, with no contribution from scattering angles in between these extremes. The results in Fig. 5, and especially for the oblate spheroid since the zone occurs near the caustic focus, imply that Newton's zero order caustic leads to the detection of angle-dependent scattered light in a manner that can be advantageous if a small change in extinction and/or angular distribution of scattered light is of interest. An illustration of how the signal detected exiting the oblate spheroid sample can be used to differentiate a solution with scattering properties versus one without scatteringis given in the following paragraphs.

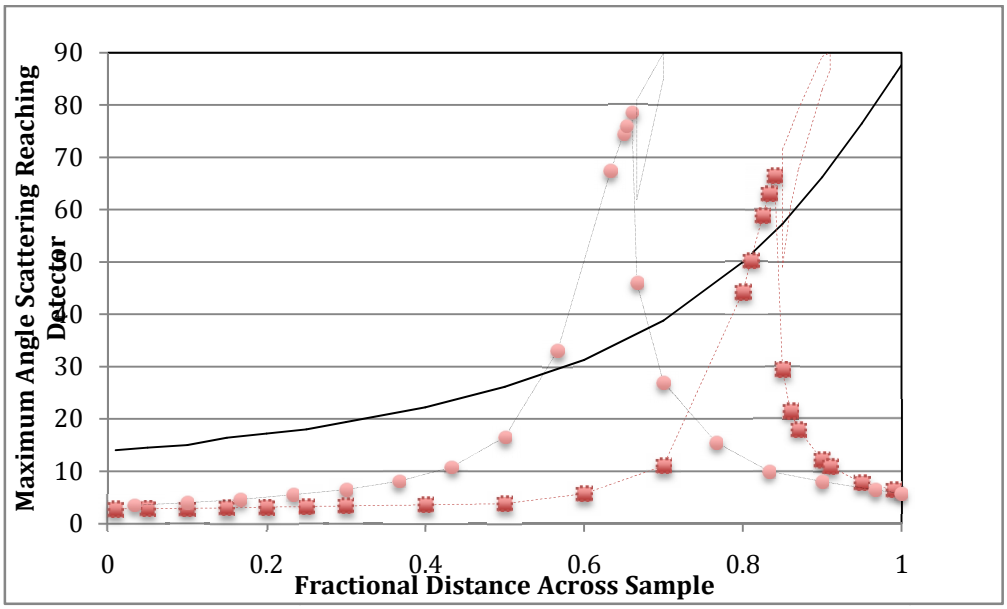

Fig. 5. Graph of ray tracing calculations for a ray traveling along the centerline for the maximum angle of light scattering that will be detected using a cuvette (solid line), spherical sample (red box with dashed line), and oblate spheroid (orange circles with dotted line). For the cuvette, the detector is placed at the wall of the cuvette. The calculated data points for the droplet are connected in order to make the trend easier to visualize. For the spheroid and sphere, there is a zone near each of the maxima, shown in the figure as trapezoids, where refracted light can reach the detector at higher angles than in the "blind spot" described in the text

For a light absorbing species such as a complexed copper ion in water, the intensity of light measured using an oblate spheroidal liquid sample at different concentrations can be directly compared to the standard means of measuring absorbance using a cuvette (Table 1). The measured values for the cuvette and spheroidal samples using photodiodes is based on measured voltage, as described in Part I of this three part series, and the reading has a standard deviation of 4%. Water is also used as a reference for the spectrometer and caustic readings given in this table. Upon dilution, each method yields values that essentially follow the Beer-Lambert law.

Table 1. Absorbance readings for clear, copper chloride solutions at concentrations well below the solubility limit. The same cuvette was used in the spectrometer and the optical platform decribed in the experimental section. Values shown are for an effective path length of 1 cm

Sample	Spectrometer (640 nm)	Cuvette (no caustic)	Spheroidal sample (caustic)
Original Conc.	0.35	0.37	0.37*
50% Dilution	0.19	0.22	0.23*

**Since the droplet is an oblate spheroid about 6 mm in diameter, the values were adjusted to a 1 cm path length measurement.*

However, when measuring light extinction of a gold nanoparticle suspension, there is a marked difference between the cuvette and spheroidal sample measurements. In Table 2, data for 10 nm gold particles are listed when using a blue (430nm) LED paired with a matched detector and for a pair of 640 nm LEDs. For the oblate spheroid sample, much less light reaches the detector using the blue LED as compared to the cuvette, while for the red LED the cuvette follows spectrophotometer readings. At 640 nm, the oblate spheroid readings do not change much with dilution. Khlebtsov and colleagues [22] calculate that for small gold nanoparticles, extinction/absorbance of light at 430-480 nm is relatively high since it is near the plasmon resonance maximum, while 90 degrees scattering intensity is weak. However, for small gold nanoparticles, the 90 degrees scattering intensity is nearly at the same intensity at 640-700 nm as at 430-480 nm, while extinction drops dramatically. It appears that the results of Table 2 are indicative of this transition. For the optical caustic measurements, the values for 640 nm light using the oblate spheroid do not change much upon dilution, whereas there is a large change for the blue LED which is at a wavelength nearer to the plasmon resonance maximum.

Table 2. Absorbance readings for 10 nm gold at different wavelengths and concentrations. The same quartz cuvette was used in the spectrophotometer and the photodiode platform

LED	Original Sample	Spectrometer	Cuvette with Device (no caustic)	Oblate Spheroid Sample with Device (caustic)
Blue	Original Conc.	0.60 **(400 nm)**	0.58	0.73*
Blue	29% Dilution		0.42	0.42*
Blue	55% Dilution	0.36 **(400 nm)**		
Red	Original Conc.	0.11 **(640 nm)**	0.11	0.13*
Red	29% Dilution		0.076	0.12*
Red	55% Dilution	0.066 **(640 nm)**		

**Since the droplet was a spheroid of about 6 mm diameter, the values were adjusted to a 1 cm path length measurement.*

3.5 Gold Nanoparticles

A well established protocol for tracking changes in light extinction and scattering due to aggregation of gold nanoparticles calls for adding sodium chloride to a gold nanoparticle

suspension that is only stabilized by charge repulsion. Fig. 6 illustrates how photodetector readings at 640 nm vary when 60 microliters of a 40 nm gold suspension is added to 60 microliters of a sodium chloride solutions. Readings were recorded after the sodium chloride solution was placed on the slide and aligned. For 0.0357 M NaCl, there does not appear to be any change in the light intensity reaching the detector over the 10 minutes that data were recorded. However, for higher concentrations of sodium chloride there is a rapid drop in the readings followed by a slower and slight increase in voltage readings over the course of the experiment. This concentration dependence is similar to behavior reported by Shulepov and Frens [23], and the dual kinetics of fast coagulation and slow rearrangement is also similar to observations by Khlebtsov and colleagues [24]. The marked change in light extinction can be followed by observing images of the sample at the two NaCl concentration extremes, as seen by the inserts in Fig. 6 for 430 nm incident light, imaged using a cell phone camera. The bottom insert is brighter due to a significant degree of aggregation using a 1M NaCl solution.

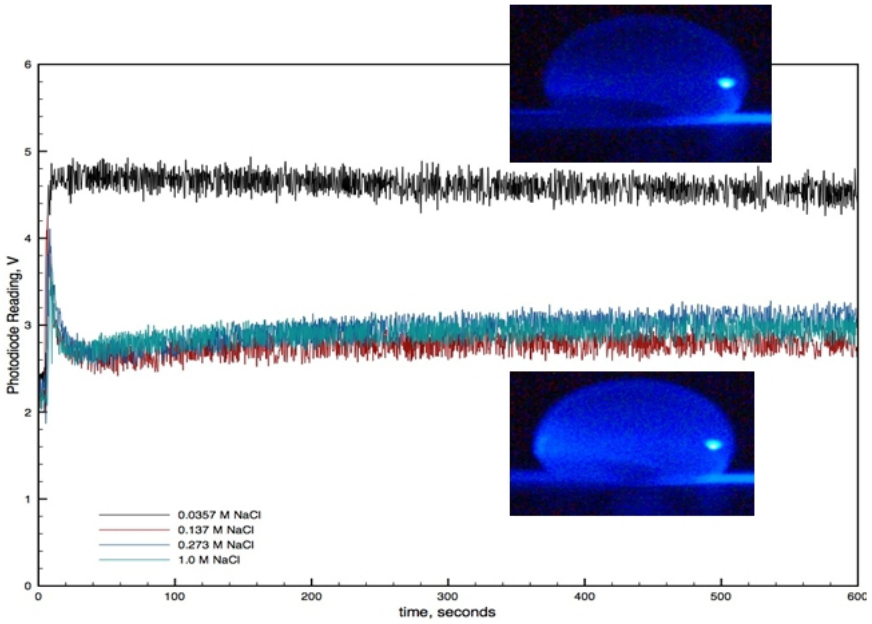

Fig. 6. Voltage readings at 10 Hz for light attenuation are shown as raw data from the data logger. Speckle images taken at 90 degree from the incident light are also shown. The top image and black line are data obtained for combining a suspension of 40 nm gold particles with 0.0357 M sodium chloride. The lower image and other lines are for combining a suspension of 40 nm gold particles with higher solution concentrations of sodium chloride. The voltage readings were initiated after 60 microliters of a sodium chloride solution is placed on the slide. Approximately 5-8 seconds afterwards, 60 microliters of an aqueous suspension of 40 nm gold was placed on the sodium chloride drop pinned to the surface. The upper insert is an image of 40 nm gold particles with no sodium chloride added, while the lower insert is an image of 40 nm gold with added 1 M sodium chloride resulting in coagulation and a higher degree of light scattering. The increase in 90 degree scattering light intensity based on these images was determined to be 168% using the integrated density software tool in Image J. The width of the droplets shown is 3 mm

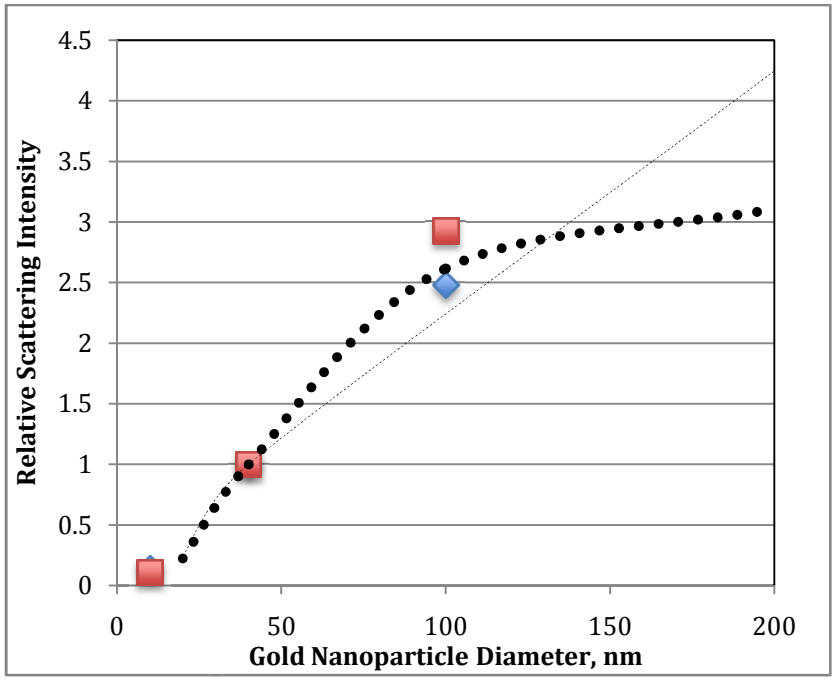

Fig. 7. 90 degree scattering imaging data for gold nanoparticles are shown in comparison to published data [25]. All data are referenced using the 40 nm gold particle intensities since the particles were obtained from the same source. The red squares are data we obtained for 640 nm light illumination, while the blue diamonds represent data we obtained using 430 nm light illumination. The published data are given as smoothed lines to differentiate them from the results of this study. The dashed line is for 470 nm excitation light, while the dotted line is for 650 nm light [19]

Aslan and colleagues [25] describe the utility of comparing the intensity of light scattered as a function of angle and gold nanoparticle size for different wavelengths of light. Since they provide data at 470 and 650 nm for gold nanoparticles from the same source as described in this article, it is useful to compare their data with our results. Fig. 7 shows a comparison of their data with data obtained at 430 and 640 nm, normalized to the intensity of the common gold nanoparticle size that was used in each study, namely 40 nm diameter. Data taken by Aslan and colleagues [25] are depicted as smooth curves. The agreement is reasonable and both measurements show that 90 degree scattering increases for larger gold nanoparticles. The calculation of integrated density was performed using background subtraction, and water was used to check for any error in reading due to light reflection. The intensity readings for water were very low and the maximum error due to reflection was less than 4%.

4. CONCLUSION

Light scattering and extinction properties of a colloidal suspension can be studied using Newton's zero order caustic generated due to a curved sample shape. High intensity light within the sample generated by shaping the suspension into an oblate spheroid leads to an optical configuration that can be used to detect light exiting the sample along the path of illumination and at 90 degrees from the incident light. Spatial autocorrelation can be used to

determine particle size for colloids that do not have a very high level of forward scattering or plasmon resonance. For nanoparticles that have extinction and scattering properties due to plasmon resonance, light exiting the sample after optical caustic focusing is modified by extinction and contains information on light scattered at small and near 90 degree angles. Due to the refraction of high intensity light within the sample, light intensity measurement as a function of gold nanoparticle concentration differs from what is measured using a standard spectrophotometer optical configuration. Imaging of the light scattered at 90 degrees using a cell phone camera complements measurement of light transmitted and provides particle size information.

ACKNOWLEDGEMENTS

The ASU Foundation provided support for this work. Support was provided to ALM by Arizona State University. We are also grateful for the helpful recommendations on the literature of optical caustics in water drops made by Prof. James Andrews of Youngstown State University.

COMPETING INTERESTS

Authors declare that no competing interests exist.

REFERENCES

1. Barth HG, Flippen RB. Particle Size Analysis. Analytical Chemistry. 1995;67:257-272.
2. Nye JF. The relation between the spherical aberration of a lens and the spun cusp diffraction catastrophe. J. Opt. A: Pure Appl. Opt. 2005;7:95-102.
3. Lock JA, McCollum TA. Further thoughts on Newton's zero-order rainbow. Am. J. Phys. 1994;62:1082-1089.
4. Lock JA. Ray Scattering by an arbitrarily oriented spheroid. II. Transmission and cross-polarization effects. Applied Optics. 1996;35(3):515-531.
5. Kofler J. Focusing of light in axially symmetric systems within the wave optics approximation, Master Thesis. University of Linz, Austria; 2004.
6. Egri A, Horváth A, Kriska G, Horváth G. Optics of sunlit water drops on leaves: conditions under which sunburn is possible. New Phytologist. 2010:185:979.
7. Haiss W, Nguyen TK, Aveyard J, Fernig DG. Determination of size and concentration of gold nanoparticles from UV-VIS spectra. Anal. Chem. 2007;79:4215-4221.
8. vanDijk MA. Nonlinear optical studies of single gold nanoparticles. Ph.D. Dissertation; 2007. Leiden University.
9. Lock JA, McCollum TA. Further thoughts on Newton's zero-order rainbow. Am. J. Phys. 1994;62:1082-1089.
10. Bateman JB, Weneck EJ, Eshler DC. Determination of particle size and concentration from spectrophotometric transmission. J. Colloid Science. 1959;14:308-329.
11. Heller W. Theoretical investigations on the light scattering of colloidal spheres. II. Accurate interpolations of theoretical turbidity-data, J. Chemical Physics. 1957;26(4):920-922.
12. Heller W. Theoretical investigations on the light scattering of colloidal spheres. III. Analytical expressions for turbidity approximating the performance of the Mie equations prior to the first maximum, J. Chemical Physics. 1957:26(5):1258-1264.

13. Heller W, McCarty HJ. Theoretical investigations on the light scattering of colloidal spheres. IV. Specific turbidities in the lower microscopic range and fine structure phenomena. J. Chemical Physics. 1958:29(1):78-80.
14. Heller W, Nakagaki M, Wallach ML. Theoretical investigations on the light scattering of colloidal spheres. V. Forward scattering. J. Chemical Physics. 1959;30(2):444-450.
15. Stevenson AF, Heller W, and Wallach ML. Theoretical investigations on the light scattering of colloidal spheres. XI. Determination of size distribution curves from spectra of the scattering ratio or from depolarization spectra, J. Chemical Physics. 1961;34(5):1789-1795.
16. Wallach ML, Heller W, Stevenson AF. Theoretical investigations on the light scattering of colloidal spheres. XII. The determination of size distribution curves from turbidity spectra. J. Chemical Physics. 1961;34(5):1796-1802.
17. Chicea D. An alternative algorithm to calculate the biospeckle size in coherent light scattering experiments. Rom. Journ. Phys. 2009;54:147-155.
18. Carnibella RP, Kitchen MJ, Fouras A. Determining particle size distributions from a single projection image. Optics Express. 2012;20:15962-15968.
19. Carvalho O, Clairac B, Benderitter M, Roy L. Statistical speckle study to characterize scattering media: use of two complementary approaches. Optics Express. 2007;15:13817-13831.
20. Piederriere Y, Boulvert F, Cariou J, Le Jeune B, Guern Y, Le Brun G. Backscattered speckle size as a function of polarization: influence of particle-size and- concentration. Opt. Express. 2005;13:5030-5039.
21. Schneider J. Superhydrophobicity and its new paradigm: materials, fluids manipulation, and biological assays. Ph.D. Dissertation; 2010. Arizona State University.
22. Khlebtsov NG, Bogatyrev VA, Khlebtsov BN, Dykman LA, Englebienne P. A multilayer model for gold nanoparticle bioconjugates: application to study of gelatin and human IgG adsorption using extinction and light scattering spectra and the dynamic light scattering method. Colloid Journal. 2003;65:622-635.
23. Shulepov SY, Frens G. Surface roughness and particle size effect on the rate of perikinetic coagulation: experimental. J. Colloid Interf. Sci. 1996;182:388.
24. Khlebtsov NG, Dykman LA, Krasnov YM, Mel'nikov AG. Light absorption by the clusters of colloidal gold and silver particles formed during slow and fast aggregation. Colloid Journal. 2000;62:765-779.
25. Aslan K, Holley P, Davies L, Lakowicz JR, Geddes CD. Angular-ratiometricplasmon-resonance based light scattering for bioaffinity sensing. J. Am. Chem. Soc. 2005;127:12115-12121.

Peer-review history:
The peer review history for this paper can be accessed here:
http://www.sciencedomain.org/review-history.php?iid=318&id=7&aid=2508